Support Information for

Benchmarking the Stability of State-of-the-Art H_2O_2 Electrocatalysts under Acidic Conditions

Guilherme V. Fortunato [a,b,c, †], Daniele C. Jung [a †], Julio C. Lourenço [b,c], Pallabi Bhuyan [c], Ji Sik Choi [a,c], Xiangyu You [c], Sumin Lim [c], Michele Melchionna [d], Hikmet Sezen [e], Jan P. Hofmann [e], Paolo Fornasiero [d], Marcos R.V. Lanza [b], Marc Ledendecker [c,f*]*

[†] these authors contributed equally to this work.

[a] Department of Technical Chemistry, Technical University of Darmstadt, Peter-Grünberg-Straße 8, 64287 Darmstadt, Germany

[b] São Carlos Institute of Chemistry, University of São Paulo, Avenida Trabalhador São-Carlense 400, São Carlos, SP 13566-590, Brazil

[c] Sustainable Energy Materials, Technical University Munich, Campus Straubing, Schulgasse 22, 94315 Straubing, Germany

[d] Department of Chemical and Pharmaceutical Sciences, Center for Energy, Environment and Transport Giacomo Ciamician, INSTM Trieste Research Unit and ICCOM-CNR Trieste Research Unit, University of Trieste, Via Giorgieri 1, 34127 Trieste, Italy

[e] Surface Science Laboratory, Department of Materials- and Geosciences, Technical University of Darmstadt, Peter-Grünberg-Straße 4, Darmstadt 64287, Germany

[f] Forschungszentrum Jülich GmbH, Helmholtz-Institute Erlangen-Nürnberg for Renewable Energy (IET-2), Cauerstraße 1, Erlangen 91058, Germany

***Corresponding authors' e-mails:**
g.fortunato@tum.de (G.V. Fortunato)
marc.ledendecker@tum.de (M. Ledendecker)

Experimental setup

As shown in Figure 1, the fully automated RRDE system is composed of three main components, namely the gas-line system, the rotator unit and the potentiostat. In order to ensure a controlled gas inflow and avoid back-flow, the gas line was integrated with six magnetic valves, one for every node. Two mass flow controllers (MFC) of the model type F-201CV-200-RAD-33-V from Bronkhorst were used to control the amount, composition and pressure of the gas fed to the system. To avoid the entry of the undesired impurities into the sensitive membrane of the MFC, particulate filters with 7 nm pores were installed ahead of the MFCs (following the flow direction). The MFCs were connected to their own power supply via an RS 232 port. Their communication was guaranteed by a serial fieldbus system using RJ 45 cables combined with a power isolator to ensure that no voltage or current were transferred through the field bus system. The red terminator in the fieldbus system, indicates the beginning, while the black one marks the end. To allow the control by the LabVIEW program, one of the MFCs was connected to the computer via an RS 232 split cable. The magnetic valves are of type 6011-A02 (Bürkert). These were controlled by an inhouse made controller supplying 24 V DC via an RS 232 to USB cable. Although the gas line system supports five gases, six magnetic valves were needed since the inert gas had a special inlet. In this way, a parallel connection to the inlet of the other measurement gases (CO_2, O_2, CO, and H_2), not only allows the Nitrogen to flow simultaneously with them, but also to flush the line through which the other gases flow.

Experimental procedures

Electrode preparation

All RRDE measurements were conducted with a total electrode loading of 100 µg cm^{-2}. For Pd_{SAC}/C, Pd_{NP}/C, and $Co_{NP}@C_{N\text{-}doped}$ samples, 2 mg of dried catalyst powder was dispersed in 1 mL of ultrapure water (18 MΩ, TOC < 3 ppb, Millipore) and then sonicated using a horn sonicator (Branson, Sonic Dismembrator 150I). To form a uniform catalyst thin film, 12 µL of the catalyst ink was drop-cast onto the GC electrode and left to dry at room temperature. After drying, the catalyst-modified GC electrode was rinsed with ultra-pure water to assess adhesion and then immersed in the electrolyte solution. Electrochemical activation was performed by cycling the potential between 0.1 and 1.0 V_{RHE} at 50 mV s^{-1} until a stable profile was achieved. For Au_{NP}/C samples, we followed the protocol reported elsewhere. [1] Briefly, 3 nm Au NPs in aqueous suspensions stabilized in citrate buffer (from Nanopartz, 0.05 mg mL^{-1} Au) were mixed

with carbon black (Printex XE2B, Orion®) to prepare a 20 wt% AuNP/C catalyst ink. The ink was prepared by combining 1.13 mL of colloidal 3 nm Au NP suspension with 0.27 mg of carbon black support, followed by horn sonication. Then, 80 µL of the catalyst ink was deposited onto the GC electrode and left to dry at room temperature. After drying, the catalyst-modified GC electrode was rinsed with ultra-pure water to verify adhesion before immersion in the electrolyte solution. The sample was then electrochemically activated by CV cycling between -0.1 and 1.7 V_{RHE} at 100 mV s^{-1} for 20 cycles.

Precondition and pre-measurement treatment

Before starting the core activity measurement, 10 CV scans in 0.1 M $HClO_4$ electrolyte are performed over a wide potential range for both disk and ring electrodes. The goal is to remove any adsorbed contaminant species left over from the polishing and cleaning procedure, ensuring that all active catalytic centers are free prior to the main measurements. The electrochemical cell is saturated for 20 minutes with the desired gas, namely O_2 or N_2 (for the background currents collection).

BOL and EOL activity measurement

The core measurement is represented by the RRDE polarization curves in O_2-saturated atmosphere under forced rotation, where disk and ring currents are monitored together. The disk is cycled between 0.1 and 1.0 V_{RHE} with a scan rate of 0.01 V s^{-1} and step size of 0.01 V while a constant, oxidizing potential of 1.4 V_{RHE} is applied to the ring. The rotation speed of 1600 rpm is ensured by the rotor. This measurement is repeated for three cycles, of which only the last one (the stabilized cycle) is evaluated. These RRDE measurements, taken at the beginning and at the end of the protocol, namely after the AST step, are called respectively beginning of life (BOL) and end of life (EOL).

For both BOL and EOL, the RRDE polarization curves are taken in O_2-atmosphere as well as N_2-atmosphere. The subtraction of the background CV taken in anaerobic conditions (absence of O_2 by N_2 purging) enables to distinguish the faradaic current (related only to the ORR in the potential region of interest) from the non-faradaic current (e.g., the capacitive current of the double layer charging and discharging process). The comparison between the subtracted O_2-curves measured at the BOL and EOL, enables insights in the degradation caused/triggered by the AST in terms of ORR activity and selectivity, and helps to evaluate the stability of the catalyst.

Apart from the initial and final stages of the AST, RRDE measurements have also been

taken at intermediate steps, namely after 100 and 1000 cycles. These intermediate measurements can have a crucial role in gaining deeper understanding about the stability of the catalyst and its degradation responses. This is of prime importance for the novel catalysts e.g., novel materials with low metal loading and/or a precisely defined nanostructure, that could be highly sensitive to the stress test.

Measurements in new electrolyte and cleaning procedure

Although perchloric acid is considered as a non-adsorbing or weakly adsorbing electrolyte, commercially available 70% $HClO_4$ contains trace impurities (0.1–10 ppm) of chloride, sulphate, phosphate and nitrate ions. Moreover, the long execution time of the designed protocols could lead to the decomposition of the acid and simultaneous generation of small quantities of chloride ions. During the long-lasting ASTs execution, impurities molecules and ions could adsorb on the catalyst layer, blocking the active sites, with deleterious effects on the catalyst performance.

To isolate the impact of catalyst degradation from these external factors, we conducted RRDE EOL activity measurements in a fresh electrolyte. Additionally, a revised cleaning protocol was implemented to minimize the risk of film damage and contamination. Specifically, the RRDE tip was carefully cleaned with fresh ultrapure water 2 times directly on the rotor without disassembling the electrode after replacing the electrochemical cell. This approach significantly reduced potential handling-induced contamination and damage.

The optimized protocol demonstrated its effectiveness: EOL activity curves obtained using both "used" and fresh electrolyte solutions were reproducible, confirming that cycling the disk before measurements effectively mitigated the influence of impurities. Consequently, all EOL curves presented in this study were measured using a fresh electrolyte solution, ensuring high reproducibility and reliable attribution of performance degradation solely to catalyst deterioration.

Preparation for AST 1 protocol – Chronopotentiometry

In this protocol, we access the Open-Circuit Potential (OCP) and the Operational Potential (OPP) by setting the potentiostat connected to the disk electrode in galvanostatic mode and applying either 0 mA cm^{-2} or -0.5 mA cm^{-2} current density. This helps us determine the upper and lower potential limits for the square wave voltammetry experiment. The measured

OCP and OPP depend on the catalyst deposited on the disk electrode and can vary even for catalysts with similar elemental composition, such as Pd_{SAC}/C and Pd_{NP}/C. These variations are an indication of differences in their structure.

Real-time dissolution monitoring using ICP-MS coupled with a channel flow electrochemical cell (CFC-ICP-MS)

To investigate the degradation mechanisms under open circuit potential (OCP) and applied potential conditions, real-time dissolution monitoring was performed using ICP-MS (Perkin Elmer Nexion 2000B) coupled with a homemade channel flow electrochemical cell (CFC-ICP-MS). A 10-ppb Rhodium solution was introduced as an internal standard, and 0.1 M $HClO_4$ was employed as the electrolyte. The electrolyte flow rate from the CFC to the ICP-MS was maintained at approximately 250 µL min^{-1}. For Pd_{NP}/C and Pd_{SAC}/C, dissolution measurements were carried out using a trapezoidal potential profile to simulate electrocatalytic conditions and assess the influence of H_2O_2 on catalyst stability. The applied potential was swept from 0.0 V to 1.0 V_{RHE} at a controlled scan rate (2 mV s^{-1}), followed by a potential hold at 1.0 V for 10 min before decreasing back to 0.0 V_{RHE}. Additionally, 20 potential cycles were applied between 0.2 V and 0.82 V_{RHE} following a square wave profile as in AST 1 but with a step of 10 seconds. These measurements were performed both in the absence and presence of 1 wt.% H_2O_2 (0.3 M) in the 0.1 M $HClO_4$ electrolyte for the Pd_{SAC}/C sample. In addition to the potential cycling experiments, potential step analysis was conducted for Pd_{SAC}/C to further explore the degradation mechanisms under both OCP and applied potential conditions. The electrode potential was initially held at OCP for 10 minutes to establish a stable baseline, followed by sequential potential steps at 0 V, 0.3 V, and 0.6 V vs. RHE, with each potential maintained for at least 10 minutes. After the initial OCP, 0 and 0.3 V steps, 0.1 M H_2O_2 was injected into the electrolyte to assess the influence of H_2O_2 exposure on Pd dissolution.

Table S1. Detailed sequence of experiments for the protocol AST 1 based on square wave voltammetry.

Sequence	Measurement	Electrode	Rotation (rpm)	Potential range / Current density	Scan Rate ($V\ s^{-1}$)	# of Cycles	Time (min)	Comments
Preparation	Chronopotentiometry [a,b]	Disk	-	0 mA cm^{-2}	-	-	>30	to define the upper potential limit (OCP)
				-0.5 mA cm^{-2}				to define the lower potential limit (OPP)
BOL activity and selectivity	Cyclic Voltammetry	Disk	-	0.1-1.0 V	0.05	10	-	Pre-treatment
		Ring		0.1-1.4 V	0.1	10		
	Linear Sweep Voltammetry using RRDE	Disk	1600	0.1-1.0 V	0.01	3	-	Collection of BOL curves
		Ring		1.4 V Hold				
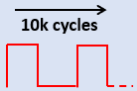	Square Wave Voltammetry	Disk	400	Upper: OCP Lower: OPP	-	10,000	-	Durability test
EOL activity and selectivity [b,c]	Cyclic Voltammetry	Disk	-	0.1-1.0 V	0.05	5	-	Pre-treatment
		Ring		0.1-1.4 V	0.1	10		
	Linear Sweep Voltammetry using RRDE	Disk	1600	0.1-1.0 V	0.01	3	-	Collection of intermediate and EOL curves
		Ring		1.4 V Hold				

OPP = operational potential

Medium: O_2-saturated 0.1 M $HClO_4$. [a] Measurement performed in galvanostatic mode.

[b] measured at 100, 1k, and 10k cycles. [c] Electrolyte changed after the experiment.

AST 1 is designed to mimic the start-stop conditions of a proton exchange membrane (PEM) H_2O_2 fuel cell (H_2O_2-FC) or a PEM H_2O_2-electrolyser with potential cycles between open circuit potential (OCP, when the device is shut down) and operational potential (OPP). The performance was evaluated before (BOL), after 100 cycles, after 1,000 cycles and after the 10,000 cycle degradation protocol (EOL). The surface of an electrocatalyst employed in an H_2O_2-producing electrochemical device is usually subjected to various harsh conditions that affect its performance and durability, especially in start-stop regimes. Depending upon the activity of the catalyst, the operational potential is theoretically expected to be lower than ca. 0.7 V_{RHE} at standard conditions, [2] while the OCP can exceed 0.9 V_{RHE}, especially for Pt- and Pd-based catalysts. [3-5] The cyclic oscillation between the operational potential (OPP) and the OCP can most likely lead to catalyst surface oxidation-reduction, resulting in electrocatalytic losses or changes in selectivity. [3-5] In addition, the degradation mechanisms such as the dissolution of both catalyst and support, agglomeration of particles and corrosion of non-noble metals at OCP on exposure to acidic electrolytes can also take place during these oscillations. [6-8]

To simulate the start-stop regime, a square wave voltammetry with 10,000 cycles of a 2-second period has been designed, and the catalyst is repeatedly cycled between two specific potential values in order to induce electrochemical degradation. The RRDE measurements have been conducted under an O_2-saturated electrolyte to limit the generation of H_2O_2 to ensure that the estimated loss of performance is solely due to the electrochemical degradation. The upper potential value corresponds to the OCP which is the maximum voltage attained when no net current is flowing through the system. The lower potential is estimated when the cathodic current density (j) value reaches -0.5 mA cm^{-2}. The current density value is set to such a low value to avoid the occurrence of the hydrogen evolution reaction (HER) and purposefully enter the mixed diffusion-kinetic region for 2e−ORR catalyst in RRDE experiment. Also, there is a likelihood that higher amount of gas will be generated which would ultimately lead to detachment of catalyst films. More details about this protocol can be found in Table S1. In AST 1, apart from the initial (BOL) and final stages (EOL) of the AST, RRDE measurements have also been taken at intermediate steps, namely after 100 and 1000 degradation cycles to measure selectivity and activity. The measurement is than performed again after 10,000 cycles (EOL). From the difference in catalytic performance between BOL and EOL, the extent of degradation can be quantified in terms of loss in activity (as substantiated from the shift of the ORR onset potential or decrease in the value of the cathodic current density at a certain potential) and changes in selectivity.

Table S2. Detailed sequence of experiments for the protocol AST 2 based on chronopotentiometry.

Sequence	Measurement	Electrode	Rotation (rpm)	Potential range / Current density	Scan Rate ($V\ s^{-1}$)	# of Cycles	Time (h)	Comments
BOL activity and selectivity	Cyclic Voltammetry	Disk	-	0.1-1.0 V	0.05	5	-	Pre-treatment
		Ring		0.1-1.4 V	0.1	10		
	Linear Sweep Voltammetry using RRDE	Disk	1600	0.1-1.0	0.01	3	-	Collection of BOL curves
		Ring		1.4 V (Hold)				
-0.5 mA cm^{-2} for 6h	Chronopotentiometry	Disk	400	-0.5 mA cm^{-2}	-	-	6h	Durability test
EOL activity and selectivity[a]	Cyclic Voltammetry	Disk	-	0.1-1.0 V	0.05	5	-	Pre-treatment
		Ring		0.1-1.4 V	0.1	10		
	Linear Sweep Voltammetry using RRDE	Disk	1600	0.1-1.0 V	0.01	3	-	Collection of EOL curves
		Ring		1.4 V (Hold)				

Medium: O_2-saturated 0.1 M $HClO_4$.

[a] Electrolyte solution changed after the previous experiment.

For AST 2, the impact of constant operation is mimicked by drawing a constant current density of -0.5 mA cm^{-2}. Towards this, the catalyst is subjected to a constant current density for 6 h, as schematically shown in Figure 3b. This protocol is designed to assess degradation mechanisms associated with sustained current load, including metal aggregation, metal dissolution, support corrosion, and changes in active site oxidation state and coordination. Additionally, under continuous operation, the generated H_2O_2 can induces chemical degradation of the catalyst or support material. However, applying larger negative current densities is not feasible with the RRDE setup, as it induces HER, which interferes with the intended evaluation. In some cases, the potential associated with this applied current density can surpass the reduction potential of the M^{x+}/M redox couple, depending on the catalyst material and its activity. This can potentially change the valence state of surface atoms and trigger structural reconstruction of the catalyst. [9] These changes may lead to undesirable changes like transformation of active sites, loss of activity, or changes in selectivity, as discussed in ref [10]. Since the electrochemically produced H_2O_2 levels are below 4 ppm, estimated by Faraday's law during AST 2, we have intuitively designed AST 3 to overcome this limitation.

Table S3. Detailed sequence of experiments for the protocol AST 3.

Sequence	Measurement	Electrode	Rotation (rpm)	Potential range / Current density	Scan Rate ($V\ s^{-1}$)	# of Cycles	Time (h)	Comments
BOL activity and selectivity	Cyclic Voltammetry	Disk	-	0.1-1.0 V	0.05	5	-	Pre-treatment
		Ring		0.1-1.4 V	0.1	10		
	Linear Sweep Voltammetry using RRDE	Disk	1600	0.1-1.0 V	0.01	3	-	Collection of BOL curves
		Ring		1.4 V (Hold)				
H_2O_2 Contact (10 mM)	OCP to prevent electrochemical H_2O_2 degradation	Disk	400	OCP	-	-	12h	Durability test in the presence of 10 mM H_2O_2 and N_2-sat
		Ring		OCP				
EOL activity and selectivity[a]	Cyclic Voltammetry	Disk	-	0.1-1.0 V	0.05	5	-	Pre-treatment
		Ring		0.1-1.4 V	0.1	10		
	Linear Sweep Voltammetry using RRDE	Disk	1600	0.1-1.0 V	0.01	3	-	Collection of EOL curves
		Ring		1.4 V (Hold)				

Medium: 0.1 M $HClO_4$ - N_2-saturated

[a] Electrolyte solution changed after the previous experiment

During the AST 3, as a caution, an almost inert condition for the RRDE electrodes is required during this measurement to prevent H_2O_2 decomposition. Specifically, the disk- and ring-electrode potentials are kept at the OCP while the electrolyte solution is saturated with inert gas, to effectively prevent the possible redox reactions in the half-cell thereby eliminating the likelihood of electrochemical degradation. After exposure, the EOL RRDE polarization curves are recorded by exchanging the H_2O_2-containing electrolyte with fresh electrolyte. Within the potential range relevant to H_2O_2 electrosynthesis, the degradation behaviour is expected to vary depending on the applied potential. It is essential to emphasize that OCP conditions are highly relevant to practical device operation since catalyst layers may encounter OCP scenarios during start-up, shutdown, or intermittent exposure to H_2O_2-rich environments. Therefore, degradation studies conducted at OCP are crucial for understanding real-world degradation mechanisms that may occur even when external potentials are not actively applied.

Table S4. Summary of the main physicochemical characteristics as well as previously reported electrocatalytic parameters for the evaluated catalyst samples.

Catalyst	Total loading (μg cm^{-2})	Metal loading (wt./wt.)	Carbon support	Particle size (nm)	Reported H_2O_2 Selectivity (%)	OCP (V_{RHE})	V@ -0.5mA cm^{-2} after 2h (V_{RHE})	Ref.
Pd_{sac}/C	100	Pd (0.9%)	Vulcan	0.4 ± 0.1	93	0.85	0.25	*11*
Pd_{NP}/C	100	Pd (1%)	Printex L6	5.5 ± 2.0	>80	0.86	0.16	12
Au_{NP}/C	100	Au (20%)	Printex XE2B	2.5 ± 0.3	>80	0.88	0.30	*1*
$Co_{NP}@C_{N\text{-}doped}$	100	Co (6%)	N-doped graphitic carbon*	10.5 ± 1.3 28.5 ± 2.1	~ 100	0.85	0.34	*13*

Defining metrics

In order to have a more in-depth view of catalyst stability, we have defined some quantifiable parameters to provide a more precise comparison between different catalysts. The following parameters can be easily collected from the LSV curves:

- Current density at the disk at a chosen potential (in this investigation, j_d at 0.2 V_{RHE} / mA cm^{-2});
- Onset potential (E_{onset} / V_{RHE});
- H_2O_2 selectivity (S_{H2O2} / %).

By comparing the LSV curves of the EOL and BOL samples, one can observe that the AST protocols decrease the disk currents. Since the idea of these protocols is not only to observe the degradation mechanism but to evaluate the stability among different catalysts subjected to the same AST protocol, it is reasonable to use the current loss between BOL and EOL samples, providing a clear indication of which catalyst performs better or worse in this regard.

In electrochemical reactions, the onset potential represents the lowest overpotential (E_{onset}) value at which a reaction product is formed at a given electrode under defined conditions. A decrease in the catalytic performance usually results in a shift of the onset potential (and, in general, of the whole ORR V-I curve) to more negative values since higher overpotentials are required to reach the same current value. Consequently, another way to evaluate the effects of the degradation protocol on the materials is by examining the E_{onset} difference between observed EOL and BOL samples. This parameter provides additional insights into the overpotential required to initiate the ORR.

Another valuable method for evaluating the degradation protocols is by comparing the selectivity of the EOL and BOL samples. The bare support, lacking any reaction at the applied potential, exhibits no current on the disk electrode, and no H_2O_2 is formed. Therefore, if dissolution is the main degradation mechanism, the ring and disk current should decrease in a proportional way, without affecting the selectivity. However, assessing this parameter remains important, particularly when considering functional groups and synergistic effects. If the AST protocols lead to the degradation of functional groups, it may result in a loss of selectivity while maintaining disk currents but decreasing ring currents.

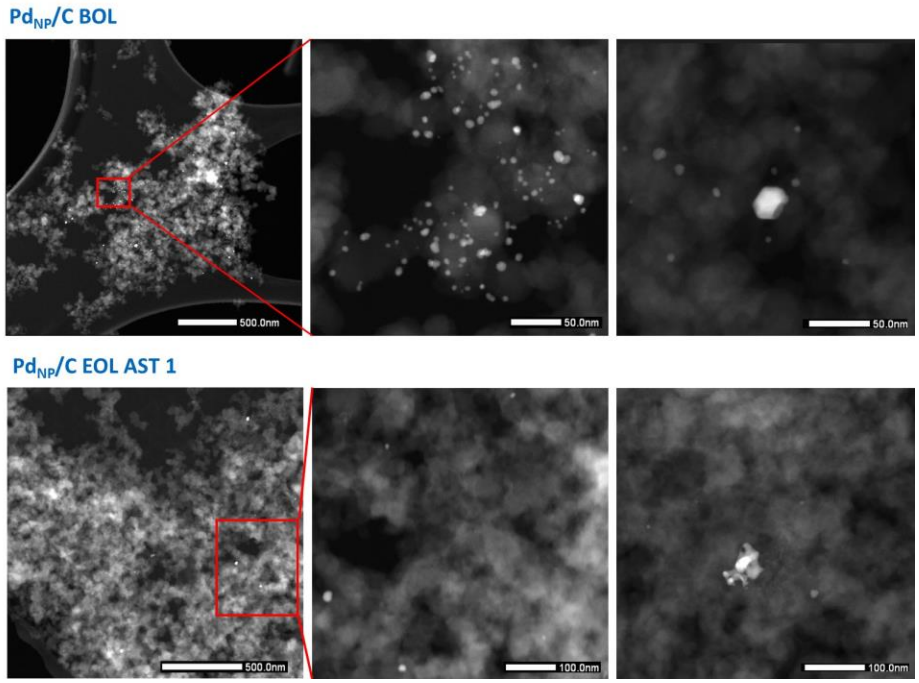

Figure S1. STEM images obtained at the BOL and EOL AST 1 stages for the Pd_{NP}/C catalyst.

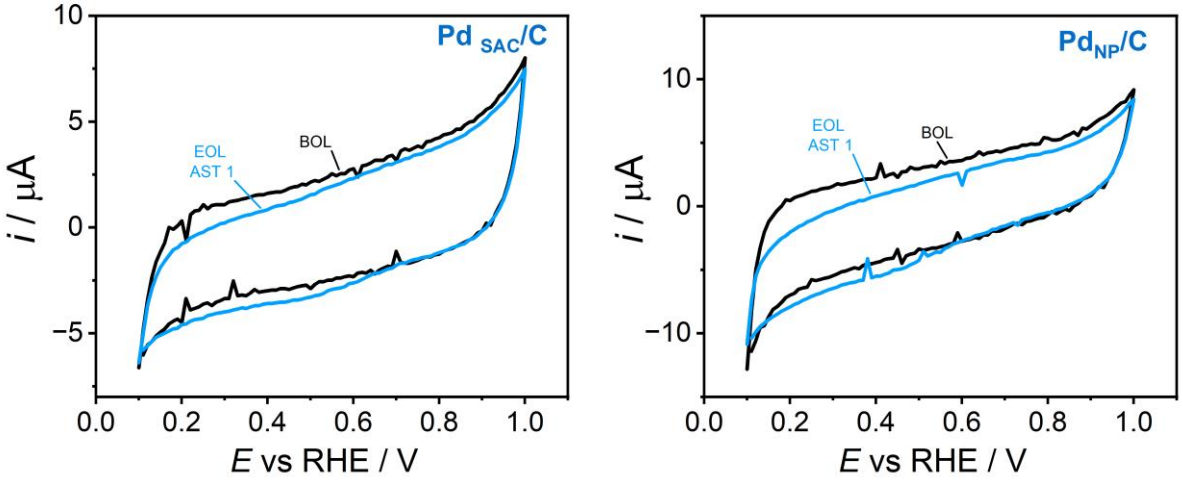

Figure S2. CV obtained at 50 mV s^{-1} in N_2-saturated 0.1 M $HClO_4$ before and after AST 1. Scans initiated at 0.1 V.

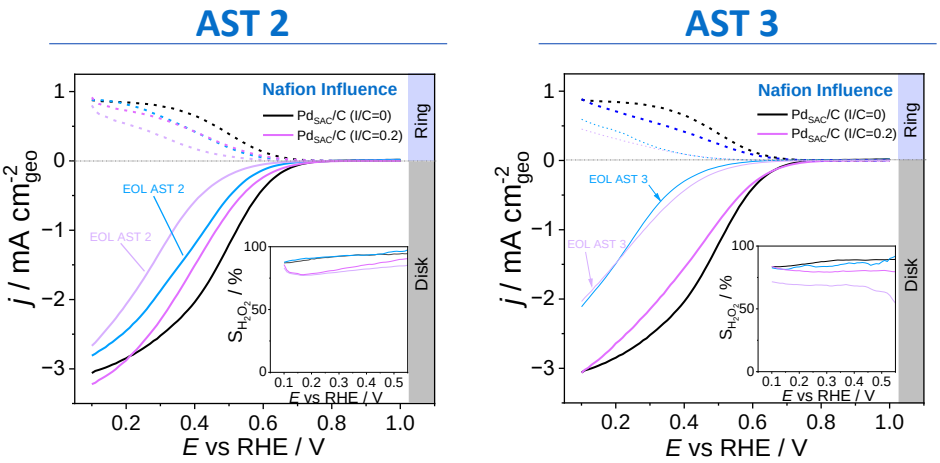

Figure S3. RRDE linear sweep voltammetry results obtained before and after AST protocols for Pd_{SAC}/C catalyst with a total loading of for 100 µg cm^{-2}, with and without Nafion binder, on the modified GC electrodes in O_2-saturated 0.1 M $HClO_4$ (rotation speed: 1600 rpm, scan rate: 10 mV s^{-1}). Scans were initiated at 0.1 V. (Inset) Percentage of H_2O_2 ($S_{H_2O_2}$) produced during the ORR at varying potentials, derived from the corresponding RRDE data. A relatively low ionomer-to-catalyst (I/C) ratio was selected to minimize mass transport limitations, as higher ionomer content can hinder the diffusion of reactants and products within the catalyst layer, [14, 15] thereby artificially reducing the observed activity and selectivity towards H_2O_2. The results demonstrate that catalyst detachment is not a significant factor contributing to the degradation trends, as similar performance decay was observed for both binder-free and Nafion-containing electrodes.

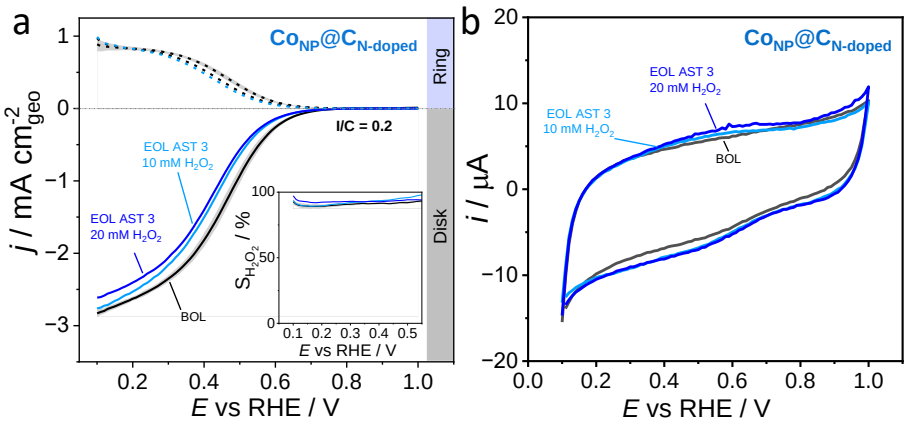

Figure S4. (a) RRDE linear sweep voltammetry results obtained before and after AST 3 for $Co_{NP}@C_{N\text{-}doped}$ catalyst with a total loading of for 100 µg cm^{-2}, with Nafion binder, on the modified GC electrodes in O_2-saturated 0.1 M $HClO_4$ (rotation speed: 1600 rpm, scan rate: 10 mV s^{-1}). Scans were initiated at 0.1 V. (Inset) Percentage of H_2O_2 ($S_{H_2O_2}$) produced during the ORR at varying potentials, derived from the corresponding RRDE data. (b) CVs obtained at 50 mV s^{-1} in N_2-saturated 0.1 M $HClO_4$ before and after AST 3. Scans initiated at 0.1 V.

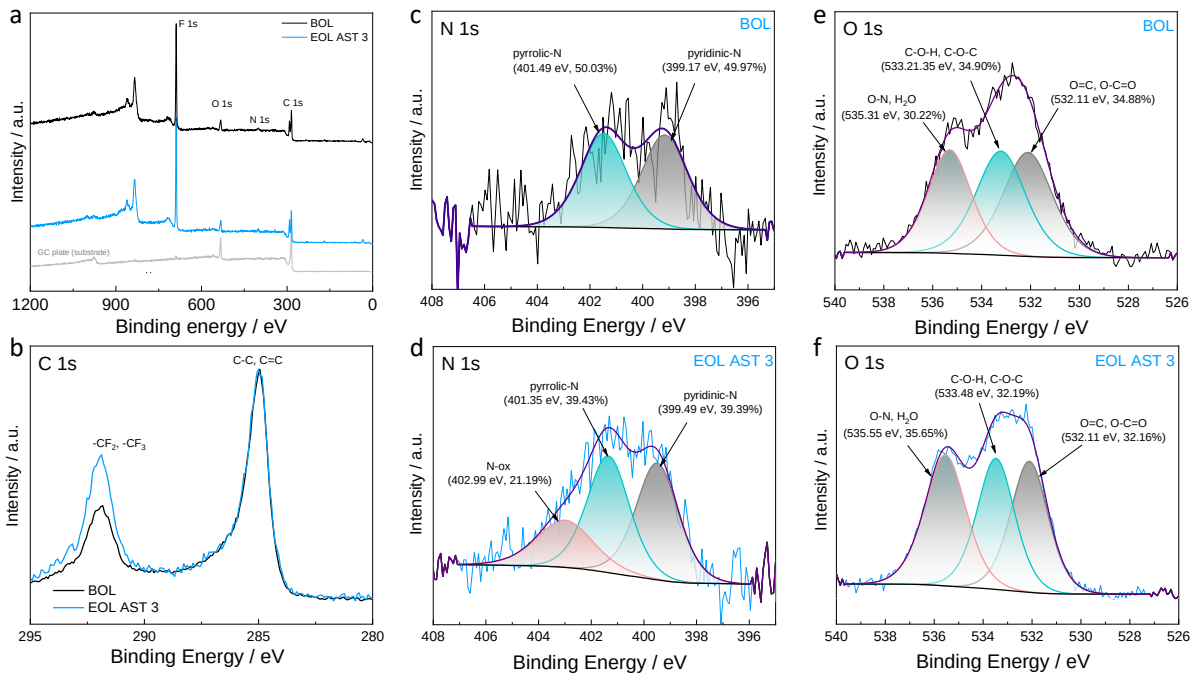

Figure S5. XPS analysis of the $Co_{NP}@C_{N\text{-}doped}$ catalyst sample before (BOL) and after AST 3 (EOL, 10 mM H_2O_2). Comparison of (a) survey, (b) C 1s, (c,d) N 1s, and (e,f) O 1s spectra reveals changes in surface chemistry induced by H_2O_2 exposure. The N 1s region shows the emergence of a peak around 403 eV after AST 3, suggesting the formation of oxidized nitrogen species (e.g., N-oxides). The O 1s spectra display increased signals attributed to C-O and O–N functionalities. The C 1s spectra show only minor changes, reflecting the relatively low sensitivity of this region to detect alterations in the carbonaceous structures. For the XPS measurements, a $Co_{NP}@C_{N\text{-}doped}$ catalyst film was prepared on a glassy carbon plate with a total loading of 400 µg cm^{-2}, using Nafion as a binder (ionomer-to-catalyst ratio = 0.2). The modified GC electrodes were tested in N_2-saturated 0.1 M $HClO_4$ according to AST 3.

References

(1) Choi, J. S.; Fortunato, G. V.; Malinovic, M.; Koh, E. S.; Aymerich-Armengol, R.; Scheu, C.; Wang, H.; Hutzler, A.; Hofmann, J. P.; Lanza, M. R. V.; et al. Decoding systematic effects and mass transport in H2O2 production via Aux/C ORR electrocatalysis. *Nano Energy* **2025**, *137*, 110811. DOI: 10.1016/j.nanoen.2025.110811.

(2) Siahrostami, S.; Verdaguer-Casadevall, A.; Karamad, M.; Deiana, D.; Malacrida, P.; Wickman, B.; Escudero-Escribano, M.; Paoli, E. A.; Frydendal, R.; Hansen, T. W.; et al. Enabling direct H_2O_2 production through rational electrocatalyst design. *Nat Mater* **2013**, *12* (12), 1137-1143. DOI: 10.1038/nmat3795.

(3) Ferreira, P. J.; la O', G. J.; Shao-Horn, Y.; Morgan, D.; Makharia, R.; Kocha, S.; Gasteiger, H. A. Instability of Pt/C electrocatalysts in proton exchange membrane fuel cells - A mechanistic investigation. *Journal of the Electrochemical Society* **2005**, *152* (11), A2256-A2271. DOI: 10.1149/1.2050347.

(4) Cherevko, S.; Keeley, G. P.; Geiger, S.; Zeradjanin, A. R.; Hodnik, N.; Kulyk, N.; Mayrhofer, K. J. Dissolution of platinum in the operational range of fuel cells. *ChemElectroChem* **2015**, *2* (10), 1471-1478. DOI: 10.1002/celc.201500098.

(5) Meier, J. C.; Galeano, C.; Katsounaros, I.; Topalov, A. A.; Kostka, A.; Schüth, F.; Mayrhofer, K. J. J. Degradation mechanisms of Pt/C fuel cell catalysts under simulated start-stop conditions. *ACS Catalysis* **2012**, *2* (5), 832-843. DOI: 10.1021/cs300024h.

(6) Kolle-Görgen, E.; Fortunato, G.; Ledendecker, M. Catalyst stability in aqueous electrochemistry. *Chemistry of Materials* **2022**, *34* (23), 10223-10236. DOI: 10.1021/acs.chemmater.2c02443.

(7) Hochfilzer, D.; Chorkendorff, I.; Kibsgaard, J. Catalyst stability considerations for electrochemical energy conversion with non-noble metals: do we measure on what we synthesized? *ACS Energy Lett* **2023**, *8* (3), 1607-1612. DOI: 10.1021/acsenergylett.3c00021.

(8) Imhof, T.; Della Bella, R. K. F.; Stuhmeier, B. M.; Gasteiger, H. A.; Ledendecker, M. Towards a realistic prediction of catalyst durability from liquid half-cell tests. *Phys Chem Chem Phys* **2023**, *25* (30), 20533-20545. DOI: 10.1039/d3cp02847j.

(9) Chen, Y.; Zhen, C.; Chen, Y.; Zhao, H.; Wang, Y.; Yue, Z.; Wang, Q.; Li, J.; Gu, M. D.; Cheng, Q.; et al. Oxygen functional groups regulate cobalt-porphyrin molecular electrocatalyst for acidic H_2O_2 electrosynthesis at industrial-level current. *Angew Chem Int Ed Engl* **2024**, *63* (34), e202407163. DOI: 10.1002/anie.202407163.

(10) Choi, J. S.; Fortunato, G. V.; Jung, D. C.; Lourenco, J. C.; Lanza, M. R. V.; Ledendecker, M. Catalyst durability in electrocatalytic H_2O_2 production: key factors and challenges. *Nanoscale Horiz* **2024**, *9* (8), 1250-1261. DOI: 10.1039/d4nh00109e.

(11) Choi, J. S.; Yoo, S.; Koh, E. S.; Aymerich-Armengol, R.; Scheu, C.; Fortunato, G. V.; Lanza, M. R. V.; Hwang, Y. J.; Ledendecker, M. Unlocking the potential of sub-nanometer Pd Catalysts for electrochemical hydrogen peroxide production. *Advanced Materials Interfaces* **2023**, *10* (36), 2300647. DOI: 10.1002/admi.202300647.

(12) Fortunato, G. V.; Kronka, M. S.; dos Santos, A. J.; Ledendecker, M.; Lanza, M. R. V. Low Pd loadings onto Printex L6: Synthesis, characterization and performance towards H_2O_2 generation for electrochemical water treatment technologies. *Chemosphere* **2020**, *259*. DOI: 10.1016/j.chemosphere.2020.127523.

(13) Filippi, J.; Miller, H. A.; Nasi, L.; Pagliaro, M. V.; Marchionni, A.; Melchionna, M.; Fornasiero, P.; Vizza, F. Optimization of H_2O_2 production in a small-scale off-grid buffer layer flow cell equipped with cobalt@N-doped graphitic carbon core-shell nanohybrid electrocatalyst. *Materials Today Energy* **2022**, *29*, 101092. DOI: 10.1016/j.mtener.2022.101092.

(14) Lauf, P.; Lloret, V.; Geuß, M.; Collados, C. C.; Thommes, M.; Mayrhofer, K. J. J.; Ehelebe, K.; Cherevko, S. Characterization of oxygen and ion mass transport resistance in

fuel cell catalyst layers in gas diffusion electrode setups. *Journal of The Electrochemical Society* **2023**, *170* (6), 064509. DOI: 10.1149/1945-7111/acdafb.
(15) Zhu, J.; Pedersen, A.; Kellner, S.; Hunter, R. D.; Barrio, J. Impact of ionomers on porous Fe-N-C catalysts for alkaline oxygen reduction in gas diffusion electrodes. *Communications Chemistry* **2025**, *8* (1), 27. DOI: 10.1038/s42004-025-01422-4.